INTERNATIONAL JOURNAL FOR NUMERICAL AND ANALYTICAL METHODS IN GEOMECHANICS
Int. J. Numer. Anal. Meth. Geomech., 2005; **29**:249–267
Published online in Wiley InterScience (www.interscience.wiley.com). DOI: 10.1002/nag.413

Unsaturated slope stability analysis with steady infiltration or evaporation using elasto-plastic finite elements

D. V. Griffiths*,† and N. Lu

Division of Engineering, Colorado School of Mines, U.S.A.

SUMMARY

The paper presents results of unsaturated slope stability analyses using elasto-plastic finite elements in conjunction with a novel analytical formulation for the suction stress above the water table. The suction stress formula requires four parameters, three for the soil type and one for the steady infiltration (or evaporation) due to environmental effects. The suction stress approach enables the analysis to proceed in the context of classical effective stress, while maintaining the advantages of a general non-linear finite element approach in which no advance assumptions need to be made about the shape or location of the critical failure surface. The results show the extent to which suctions above the water table can increase the factor of safety of a slope for a variety of different soil types and infiltration rates. All stability analyses that include the effects of suction stresses are contrasted with more traditional approaches in which water pressures above the water table are ignored. Copyright © 2005 John Wiley & Sons, Ltd.

KEY WORDS: unsaturated; pore suctions; effective stress; slope stability; finite elements; elasto-plasticity

INTRODUCTION

It has long been known that pore suctions in unsaturated soils can play an important role in the stability of geotechnical structures (e.g. References [1–5]), at least temporarily, and that these suctions are highly dependent on soil type and infiltration conditions. In this paper, the factor of safety of unsaturated soil slopes is examined using elasto-plastic (Mohr–Coulomb) finite element analysis, in conjunction with a novel theoretical approach for modelling the 1-d profile of suction stress above the water table for different soil types, and steady infiltration (or evaporation) conditions. The research described in this paper considers the water table elevation to be constant, however if a site-specific relationship between infiltration rate and water table height was available (e.g. Reference [6]), it could easily be included into the analyses. The initial part of the paper gives a detailed derivation of a 1-d suction theory, highlighting some of the more significant properties of the model. In the second part of the paper, the model is incorporated into an elasto-plastic finite element programme for c', ϕ' soils, including a water

*Correspondence to: D. V. Griffiths, Division of Engineering, Colorado School of Mines, U.S.A.
†E-mail: d.v.griffiths@mines.edu

Contract/grant sponsor: NSF; contract/grant number: CMS 97-13442

Received 18 June 2004
Revised 4 October 2004

table [7]. Results are obtained for the factor of safety of the slope including suction stresses above the water table, and these are compared with the more conventional approach in which water pressures above the water table are ignored. In all cases, the factor of safety is higher when suctions are included, however the sensitivity of the factor of safety to the presence of suctions is shown to be highly dependent on the water table elevation, the soil type and infiltration conditions.

SUCTION STRESS FORMULATION

The formulation is based firmly within the context of Terzaghi's classical effective stress theory as modified for unsaturated soils by Bishop [8] in the form:

$$\sigma' = (\sigma - u_a) + \chi(u_a - u_w) \tag{1}$$

in which σ' and σ are, respectively, the effective and total stresses, u_a is the air pressure in the voids, and u_w is the suction pore pressure within the unsaturated soil matrix. The term $(u_a - u_w)$ is called the *matric suction*, and χ is the matric suction coefficient, generally determined experimentally, which is related primarily to the degree of saturation of the soil [9–13]. The matric suction coefficient χ may be interpreted as the average proportion of the voids cutting any cross-section through a partially saturated soil, that passes through water. In relation to Equation (1), χ describes the proportion of the matric suction that is directly translated to the soil skeleton in the form of effective stress. It is clear from Equation (1) that pore suctions will *increase* the effective stress between soil particles. Consideration of a couple of special cases however, shows that for a saturated soil ($S = 1$), and $\chi = 1$, hence the classical effective stress equation for compressive pore pressures is retrieved as:

$$\sigma' = \sigma - u_w \tag{2}$$

and for a completely dry soil ($S = 0$), $\chi = 0$, leading to:

$$\sigma' = \sigma - u_a \tag{3}$$

From Equation (3), effective and total stresses are essentially equal, because in the current paper it will be assumed that $u_a \approx 0$. The exception to this might only occur under experimental conditions, when u_a has been increased in the laboratory to facilitate the measurement of matric suction.

The theory proposed in this paper leads to a closed form expression for the *suction stress* given by $\chi(u_a - u_w)$. From Equation (1), the suction stress is the critical parameter for modelling the mechanical properties of unsaturated soil, since it directly influences the effective stress. Since the suction stress consists of the product of two terms, the subsequent theory deals with each term separately, before combining them in a powerful general expression.

Derivation of the profile of matric suction $(u_a - u_w)$

We start with Darcy's law for 1-d steady seepage,

$$q = -k\frac{\mathrm{d}h}{\mathrm{d}z} \tag{4}$$

where q is the flow rate (per unit area), k is permeability, h is the total head, and z is a depth co-ordinate equal to zero at the water table. Equation (4) gives that negative q implies infiltration or steady seepage towards the water table, and positive q implies evaporation or steady seepage away from the water table.

The total head consists of pressure and elevation components, where:

$$h = \psi + z \tag{5}$$

and ψ is the (negative) suction pressure head given by:

$$\psi = \frac{-(u_a - u_w)}{\gamma_w} \tag{6}$$

and γ_w is the unit weight of water.

A simple expression for the permeability of an unsaturated soil as a function of its matric suction and saturated permeability k_s, has been proposed by Gardner [14] where:

$$k = k_s e^{-\alpha(u_a - u_w)} \tag{7}$$

in which α is the inverse of the air entry pressure (in kPa^{-1}) and typically lies in the range $0.001 < \alpha < 0.5\ kPa^{-1}$ ([15–18]). The air entry pressure is the matric suction value that must be exceeded before air recedes into the soil pores.

Equation (4) may thus be written as:

$$q = -k_s e^{-\alpha(u_a - u_w)} \left(-\frac{1}{\gamma_w} \frac{d(u_a - u_w)}{dz} + 1 \right) \tag{8}$$

Further rearrangement, leads to the ordinary differential equation:

$$\frac{d(u_a - u_w)}{dz} = \gamma_w \left(\frac{q}{k_s} e^{\alpha(u_a - u_w)} + 1 \right) \tag{9}$$

and inserting the boundary condition at the water table, $(u_a - u_w) = 0$ when $z = 0$, leads to the solution for the matric suction as a function of z and q, and the material parameters k_s, α and γ_w for steady 1-d flow.

$$(u_a - u_w) = -\frac{1}{\alpha} \ln \left[\left(1 + \frac{q}{k_s} \right) e^{-\alpha \gamma_w z} - \frac{q}{k_s} \right] \tag{10}$$

The properties of this equation once it has been further developed to include the influence of χ will be discussed later in this paper.

Derivation of matric suction coefficient, χ

The derivation now makes use of the soil water characteristic curve (SWCC), frequently referred to in unsaturated soil mechanics (e.g. Reference [4]). The SWCC varies widely for different soil types (e.g. References [14, 18, 19]) and is often considered a unique property that distinguishes one soil from another. In this study, the van Genuchten [19] model is used in which the effective degree of saturation is expressed as follows:

$$\frac{S - S_r}{1 - S_r} = \left(\frac{1}{1 + (\alpha(u_a - u_w))^n} \right)^{(n-1)/n} \tag{11}$$

where S is the degree of saturation and S_r is the residual degree of saturation which is defined as the degree of saturation at which an increase in matric suction does not produce a significant

change in the degree of saturation. The parameter n is an exponent relating to pore size. Typical values of n for a wide range of soils have been shown (e.g. References [18, 19]) to lie in the range $1.1 < n < 8.5$.

The matric suction coefficient χ has been examined experimentally and theoretically as a function of the matric suction or degree of saturation (e.g. References [11, 13, 20–23]). The matric suction coefficient χ as indicated in Equation (1), has been shown from experiments (e.g. Reference [12]) to be approximately modelled by making it equal to the effective degree of saturation, thus:

$$\chi = \frac{S - S_r}{1 - S_r} \tag{12}$$

and

$$\chi = \left(\frac{1}{1 + (\alpha(u_a - u_w))^n} \right)^{(n-1)/n} \tag{13}$$

Substitution of the expression for matric suction from Equation (10) into Equation (13) gives:

$$\chi = \left(\frac{1}{1 + (-\ln[(1 + q/k_s)e^{-\alpha\gamma_w z} - q/k_s])^n} \right)^{(n-1)/n} \tag{14}$$

General equation for suction stress, $\chi(u_a - u_w)$

The general equation for the suction stress, is given by combining Equations (10) and (14) as follows:

$$\chi(u_a - u_w) = \frac{-\ln[(1 + q/k_s)e^{-\alpha\gamma_w z} - q/k_s]}{\alpha(1 + (-\ln[(1 + q/k_s)e^{-\alpha\gamma_w z} - q/k_s])^n)^{(n-1)/n}} \tag{15}$$

Application of Equation (15) will clearly be strongly influenced by soil type and climate, so typical values of soil parameters and infiltration/evaporation rates (e.g. Reference [24]) are given in Tables I and II, respectively.

Dimensionless form of the suction stress equation

To generalize the equation for all soil types and infiltration rates, and to facilitate analysis of the model, Equation (15) has been rearranged in dimensionless form as follows:

$$U = \frac{-\ln[(1 + Q)e^{-Z} - Q]}{[1 + (-\ln[(1 + Q)e^{-Z} - Q])^n]^{(n-1)/n}} \tag{16}$$

Table I. Typical ranges of unsaturated soil parameters for various soils.

Soil type	n	α (kPa^{-1})	S_r (%)	k_s (m/s)
Sand	4–8.5	0.1–0.5	5–10	10^{-2}–10^{-5}
Silt	2–4	0.01–0.1	8–15	10^{-5}–10^{-9}
Clay	1.1–2.5	0.001–0.01	10–20	10^{-9}–10^{-13}

Table II. Typical range of infiltration (−) and evaporation (+) rates.

Flow type	q (m/s)
High infiltration	-3.14×10^{-8}
No flow	0
High evaporation	1.15×10^{-8}

Table III. Typical ranges of dimensionless depth (Z) and infiltration (Q).

Soil type	Depth ($0 < z < 50$ m)	Infiltration
Sand	$0 < Z < 250$	$-0.003 < Q < 0.001$
Silt	$0 < Z < 50$	$-1 < Q < 10$
Clay	$0 < Z < 5$	$-1 < Q < 10\,000$

where

$$U = \alpha\chi(u_a - u_w) \quad \text{dimensionless suction stress}$$

$$Z = \alpha\gamma_w z \quad \text{dimensionless depth co-ordinate}$$

$$Q = \frac{q}{k_s} \quad \text{dimensionless infiltration}$$

Table III gives typical ranges of the dimensionless parameters Z (assuming a depth above the water table of $z = 50$ m represents an upper bound for most practical purposes) and Q for different soil types. Values of U given by Equation (16) will be discussed in the next section.

CHARACTERISTICS OF THE SUCTION STRESS EQUATION

The dimensionless suction stress from Equation (16) is a function of three independent variables, where:

$$U = f(Z, Q, n) \tag{17}$$

The characteristics of the equation are conveniently explained using the four different regimes, defined by the ranges of Q and n, as shown in Figure 1.

Regime I. ($Q \geqslant 0$ *and* $n > 2$): This regime corresponds to any level of evaporation, as indicated by a positive value of Q. Evaporation implies a steady withdrawal of water from the unsaturated zone.

By differentiation of U with respect to Z in Equation (15) it can be shown that:

$$U_{max} = \frac{(n-2)^{(n-2)/n}}{(n-1)^{(n-1)/n}} \tag{18}$$

at a depth of

$$Z_{max} = \ln\left\{\frac{(1+Q)e^{(n-2)^{-1/n}}}{1+Qe^{(n-2)^{-1/n}}}\right\} \tag{19}$$

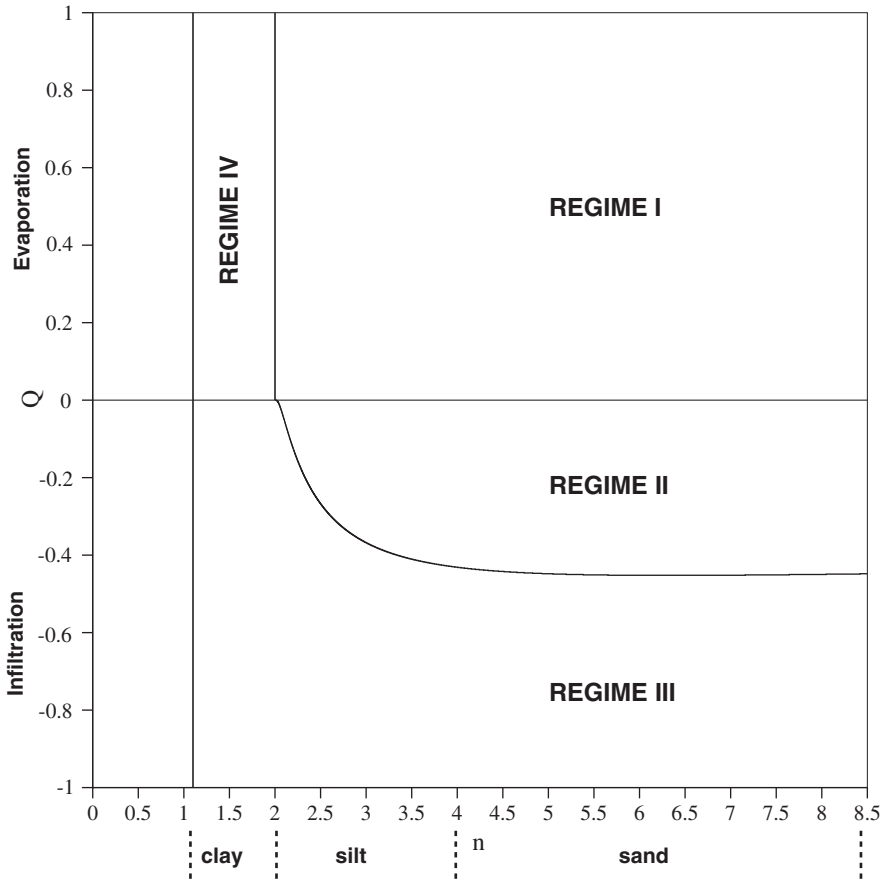

Figure 1. Characteristics regimes of the suction stress profile as a function of the pore size exponent n and the dimensionless infiltration rate Q.

All evaporative cases exhibit a limiting value of Z_{limit}, given by:

$$Z_{\text{limit}} = \ln\left\{1 + \frac{1}{Q}\right\} \tag{20}$$

where

$$U \to 0 \quad \text{as } Z \to Z_{\text{limit}} \tag{21}$$

For $Z > Z_{\text{limit}}$ the solution is mathematically undefined, however for practical purposes U can be taken to be essentially zero. For the special case of no flow ($Q = 0$) however, $Z_{\text{limit}} \to \infty$.

Figures 2(a) and 2(b) show typical results in this regime for the case of $n = 4$ and $Q = 0.8$, respectively. In Figure 2(a), the maxima are fixed at $U_{\max} = 0.6204$ from Equation (18) and $U \to 0$ as $Z \to Z_{\text{limit}}$. The Z_{limit} values are indicated on the figure. As an example, from Equation (19), when $Q = 0.4$, $Z_{\text{limit}} = 1.2528$. Although U is undefined for $Z > Z_{\text{limit}}$, it will be assumed to equal zero in this range for the purposes of the slope analyses described later in this paper.

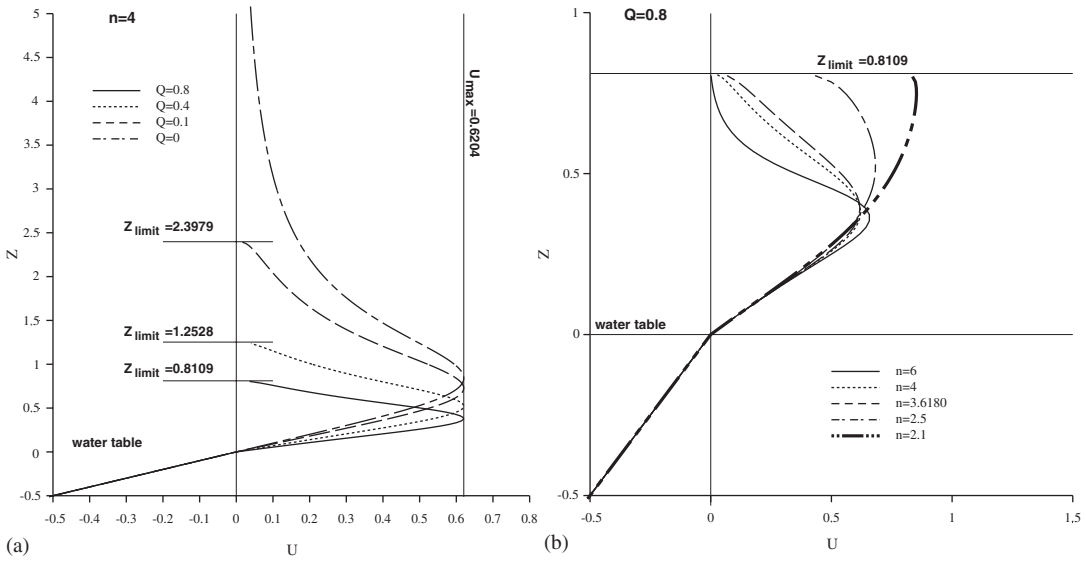

Figure 2. (a) Regime I: plots of U vs Z for the case of $n = 4$; and (b) Regime I: plots of U vs Z for the case of $Q = 0.8$. The minimum value of $U_{\max}$ occurs when $n = (5 + \sqrt{5})/2 = 3.6180$. The limiting Z value is indicated.

The linear region corresponding to $Z<0$ represents the simple hydrostatic (compressive) pressure profile beneath the water table. It may be noted that the no-flow case ($Q = 0$) is sometimes referred to as 'hydrostatic', because the suctions above the water table are initially a linear extrapolation of the hydrostatic compressive pressures below.

The influence of n on the suction profile in this regime is shown in Figure 2(b). By differentiating Equation (18) with respect to n, it is easily shown that $U_{\max}$ reaches a minimum value of 0.6180 when $n = (5 + \sqrt{5})/2 = 3.6180$. The figure also indicates that for the case of $Q = 0.8$, the suction stresses are quite insensitive to n between the water table and $Z_{\max}$, but considerably more sensitive above $Z_{\max}$.

Regime II. ($-e^{-(n-2)^{-1/n}} < Q < 0$ *and* $n > 2$): This regime corresponds to 'small' steady infiltration into the unsaturated zone, as indicated by a negative value of Q.

The maximum suction stress $U_{\max}$, has the same magnitude, and occurs at the same depth $Z_{\max}$ as given by Equations (18) and (19) in Regime I.

After passing the peak however,

$$U \to U_{\text{limit}} \tag{22}$$

where

$$U_{\text{limit}} = \frac{-\ln\{-Q\}}{[1 + (-\ln\{-Q\})^n]^{(n-1)/n}} \quad \text{as } Z \to \infty \tag{23}$$

thus the asymptotic value of U is a function of both Q and n in this regime.

Figure 3(a) shows some typical results in this regime for the case of $n = 4$. The maxima are fixed at $U_{\max} = 0.6204$ as before from Equation (18) and U tends asymptotically to the values given by Equation (23). The figure indicates that the suction stress above $Z_{\max}$ climbs quite

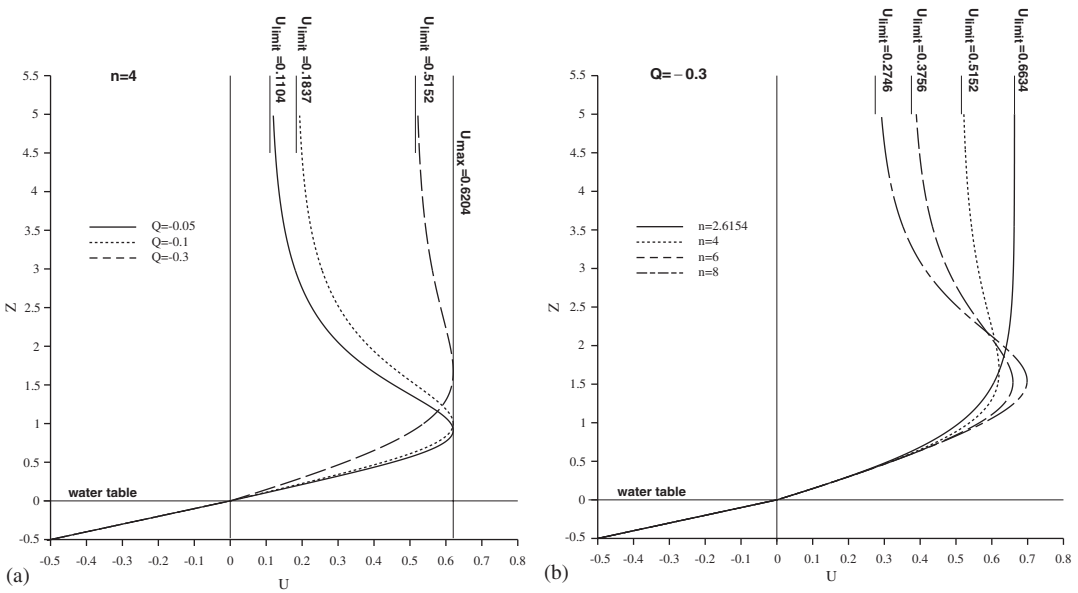

Figure 3. (a) Regime II: plots of U vs Z for the case of $n = 4$. Asymptotic values of U are indicated; and (b) Regime II: plots of U vs Z for the case of $Q = -0.3$. Asymptotic values of U are indicated.

rapidly as the infiltration rate Q increases. For an infiltration rate given by $Q = -0.3$. Figure 3(b) shows the influence of n on the suction stress. As in Regime I, the suction stresses become more sensitive to n at depths greater than the maximum depth $Z_{\max}$. The limiting value of n for this regime with $Q = -0.3$ is given by $n = 2.6154$. In this case, the suction stress tends monotonically to its maximum value of $U_{\max} = 0.6634$.

Regime III. ($-1 < Q < 0$ *and* $1.1 < n < 2$) *or* ($-1 < Q \leqslant -\mathrm{e}^{-(n-2)^{-1/n}}$ *and* $n \geqslant 2$): This regime corresponds to 'large' steady infiltration into the unsaturated zone, as indicated by negative values of Q going down to the theoretical limit of -1. In this regime, the suction stresses exhibit no maxima, but tends to the same asymptotes as defined by Equation (23) in Regime II.

Figure 4(a) shows some typical results in this regime for the case of $n = 4$. It should be noted that as the infiltration Q increases, the suction stress above the water table falls quite rapidly, tending to zero as Q tends to its lower limit of $Q \to -1$. The upper limit of Q in this regime for $n/ge2$, is given by $Q = -\mathrm{e}^{-(n-2)^{-1/n}} = 0.4313$. In this case the asymptotic value of the suction stress is $U_{\max} = 0.6204$, which is the same as the maximum value observed in Regimes I and II for $n = 4$ and given by Equation (18).

Figure 4(b) for the case of $Q = -0.7$, shows the interesting result that the suction stress in this regime is quite insensitive to the value of n. The value of U_{limit} indicated in the figure corresponds to $n = 4$.

Regime IV. ($Q \geqslant 0$ *and* $1.1 < n \leqslant 2$): This is the 'dry clayey soil' evaporative case in which the suction stresses can theoretically become very large. As in all evaporative cases (Regimes I and IV), the solution is only defined for $Z < Z_{\text{limit}}$ from Equation (20). The character of the limiting value of U in Regimes I and IV is quite different however. In Regime IV, the suction stresses

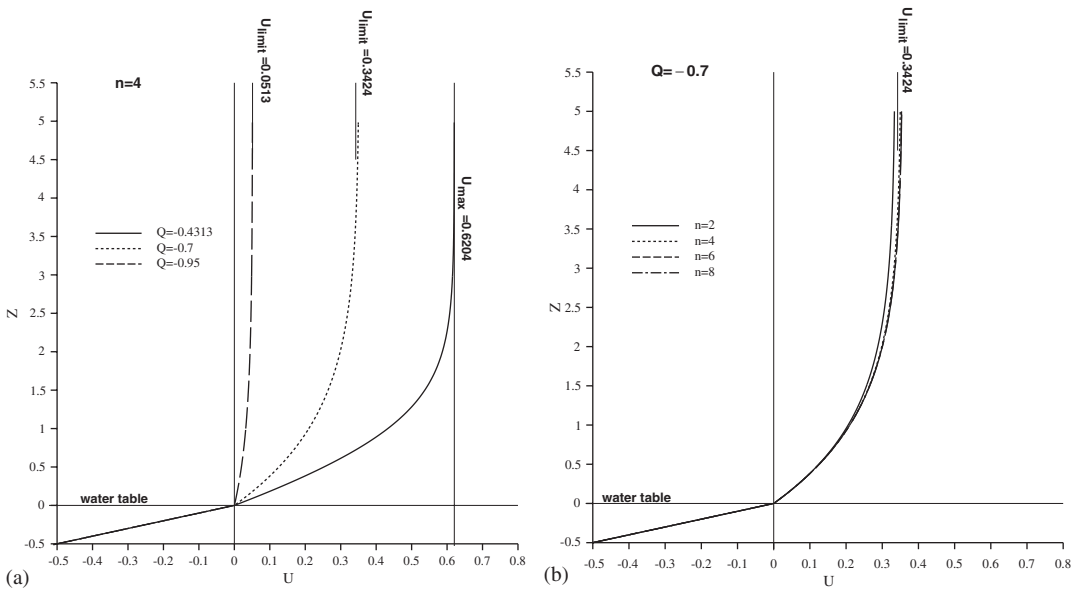

Figure 4. (a) Regime III: plots of U vs Z for the case of $n = 4$. Asymptotic values of U are indicated; and (b) Regime III: plots of U vs Z for the case of $Q = -0.7$. Asymptotic value of U corresponding to $n = 4$ is indicated.

increase steadily with depth to the following limits:

$$\begin{aligned} &\text{As} \quad Z \to Z_{\text{limit}} \\ &\text{if} \quad n = 2, \quad U \to 1 \\ &\text{else if} \quad 1.1 < n < 2, \quad U \to \infty \end{aligned} \tag{24}$$

The behaviour of the suction stress above the water table is indicated in Figure 5(a) for the case where $n = 1.7$, and in Figure 5(b) for the case where $Q = 0.8$. The sensitivity of the suction stress to the evaporation rate Q is clearly indicated in Figure 5(a), and is a characteristic in this regime that has been observed by others (e.g. References [17, 25, 26]). The very rapid increase in the suction stress above the water table as the evaporation rate increases should be noted. The asymptotic behaviour of $U \to \infty$ as $Z \to Z_{\text{limit}}$ for $n < 2$ is clearly shown in both figures, although Figure 5(a) also shows the special limiting case when $n = 2$, in which $U \to 1$.

Review of the role of infiltration on suction stresses

This section summarizes the influence of infiltration on the suction stress profile for two soil types. In the first case shown in Figures 6(a) and 6(b), the pore size exponent is held constant at $n = 1.7$, implying a clay, while Q is varied systematically in the range -0.95 (infiltration) $< Q < 0.95$ (evaporation). From Figure 1, this range of properties cuts through Regimes III and IV. The general trend for this soil type from Figure 6(a), is that as the evaporation decreases and the infiltration increases, the suction stresses are reduced and eventually die away to zero. For

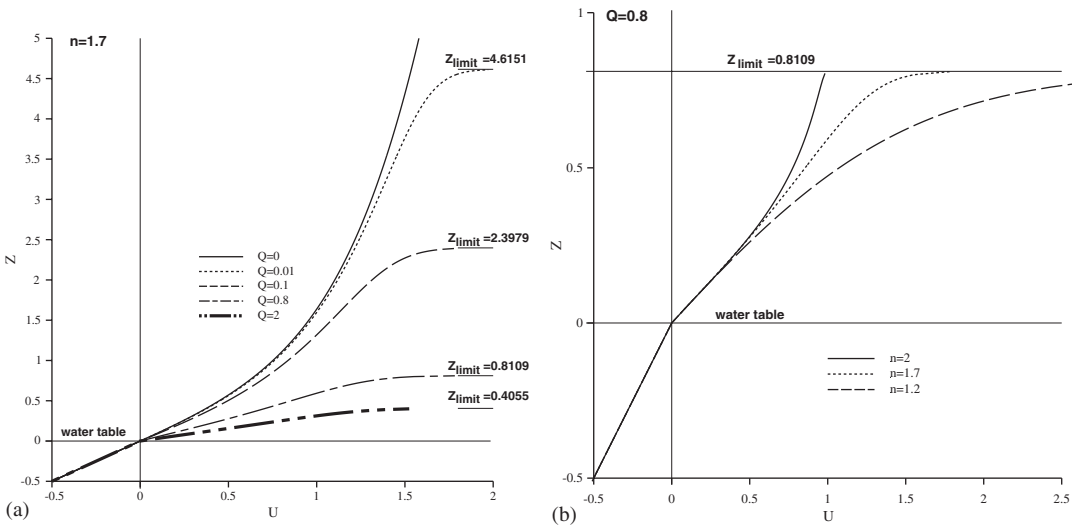

Figure 5. (a) Regime IV: plots of U vs Z for the case of $n = 1.7$. Limiting Z values are indicated; and (b) Regime IV: plots of U vs Z for the case of $Q = 0.8$. Limiting Z value is indicated.

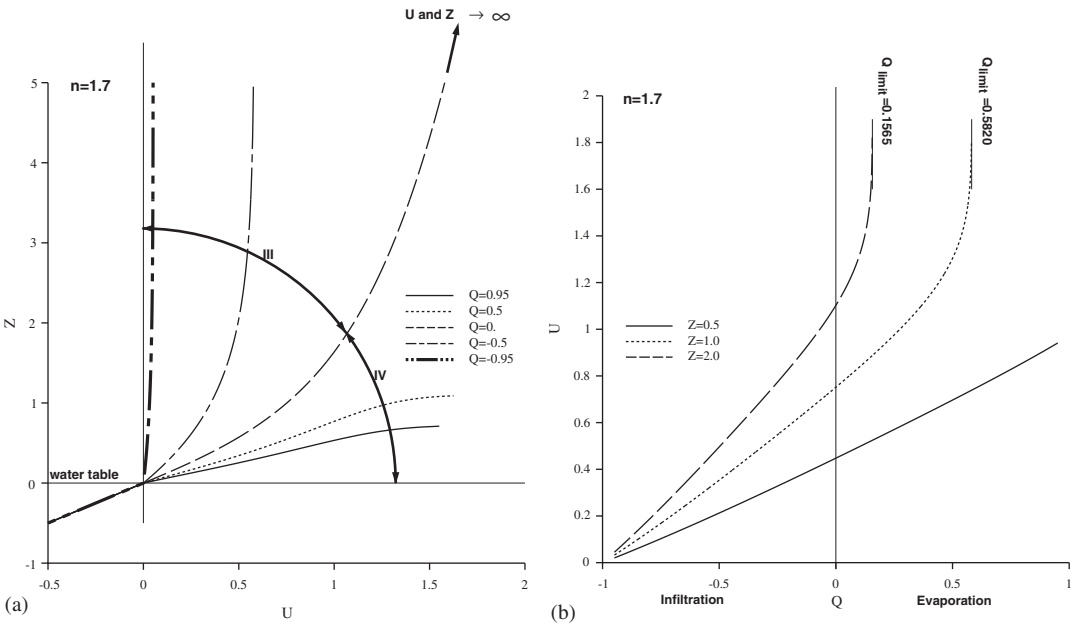

Figure 6. (a) Influence of Q on the suction profile for $n = 1.7$; and (b) Plot of Q vs U at fixed depths for $n = 1.7$.

the same soil type, Figure 6(b) shows how the suction stress varies with Q for different values of the depth variable Z. It is shown that as long as Q corresponds to infiltration, the relationship between U and Q is essentially linear, however at greater depths and with evaporation, the

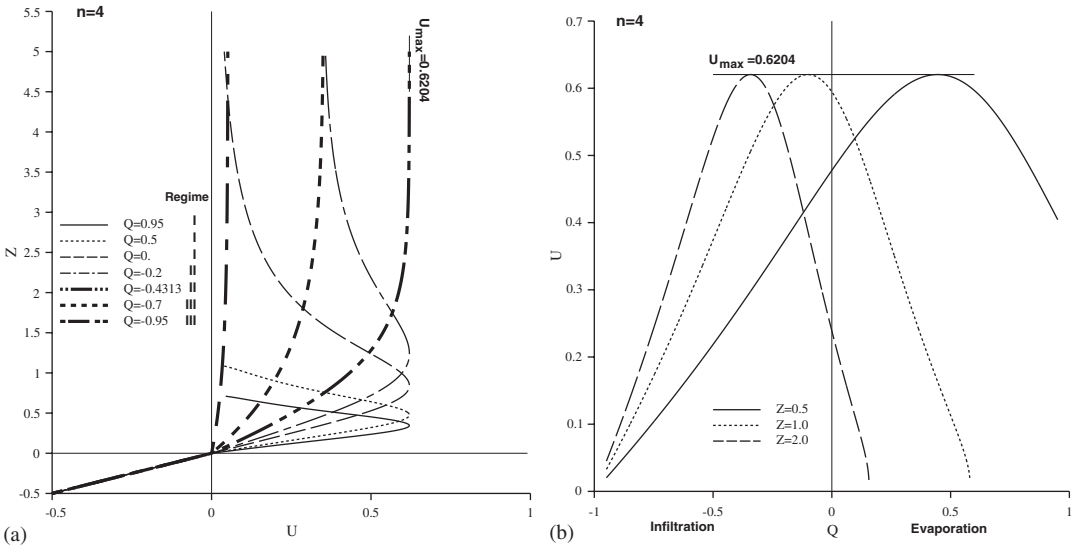

Figure 7. (a) Influence of Q on the suction profile for $n = 4$; and (b) Plot of Q vs U at fixed depths for $n = 4$.

suction stress increase very rapidly, tending to infinity at a limiting value of $Q = Q_{\text{limit}}$ given from Equation (20).

In the second case shown in Figures 7(a) and 7(b), the pore size exponent is held constant at $n = 4$, implying a borderline silt/sand. From Figure 1, this range of properties cuts through Regimes I–III. The trend for this soil type shown in Figure 7(a) is clearly quite complex, with the suction stress showing significant sensitivity to the infiltration level Q. For the same soil type, Figure 7(b) shows how the suction stress varies with Q for different values of the depth variable Z. For any given depth above the water table, a 'wave' of suction stress is obtained, which starts and finishes at zero, corresponding to high evaporation and high infiltration levels. In between these zero values, lies a maximum suction stress level given by Equation (18). The flow rate Q at which the maximum occurs tends to be in the evaporative range for smaller values of Z, and in the infiltrative range for higher values of Z. This interesting result implies that for coarser-grained soils at greater depths above the water table, a modest increase in the infiltration level from zero can *increase* the suction stress levels. For modest infiltration levels, this is due to the increased water contact areas between the particles more than compensating for the falling suctions, resulting in a net increase in suction stress.

In all cases and depths, large infiltration rates drive the suction stresses to zero, as shown in Figures 6(b) and 7(b).

FINITE ELEMENT IMPLEMENTATION

In this section of the paper, the suction stress formulation described previously, is incorporated into the elasto-plastic finite element slope stability analysis technique described in detail by Griffiths and Lane [7].

The finite element approach to slope stability analysis is gaining acceptance, as a robust and accurate alternative to classical limit equilibrium methods. One of the main benefits of finite element slope stability analysis, is that no *a priori* decision needs to be made by the user as to the shape or location of the critical failure surface. In the finite element approach, the critical failure mechanism develops along the path where the shear strength (τ_f) of the soil is unable to support the shear stress (τ) generated by gravitational loading. For further information and listings of typical programmes for finite element slope stability, the reader is referred to the text by Smith and Griffiths [27].

Another clear benefit of the finite element approach, is the ease with which different soil layers can be incorporated. Similarly, for the purposes of this study, the suction stress level within every part of the slope can be defined to a high level of resolution. At each Gauss point within each element,[‡] and for given unsaturated soil properties (α and n), infiltration rate q and depth above the water table z, the suctions stress $\chi(u_a - u_w)$ is found from Equation (15).

In practice, the location of the water table might be measured, in view of the fact that its location and rate of change will be highly dependent on the site-specific climate, soil conditions and topology.

This suction stress is then *added* to the total normal stress (σ) generated by gravitational loading, giving the normal effective stress (σ') at each Gauss point from Equation (1). The normal effective stress is then substituted to the right-hand side of Coulomb's failure law,

$$\tau_f = \sigma' \tan \phi' + c' \tag{25}$$

It is clear from Equation (25), that the presence of suction stresses will (a) increase the shear strength of the soil and hence the factor of safety, and (b) influence only the *frictional* contribution to strength.

While it is recognized that a 1-d suction theory is being combined with 2-d slope stability analysis, the authors consider this to be an acceptable simplification for an initial study. Even in conventional slope stability analysis with an inclined free-surface, the 2-d flow pattern is rarely taken into account and the flow is assumed to be horizontal, with pore pressures computed simply from the vertical height of the free-surface.

The factor of safety of a slope by finite element analysis is obtained by generating the effective stress field due to gravity and suctions as described above, followed by a systematic reduction in the shear strength parameters $\tan \phi'$ and c', until the algorithm is unable to satisfy both the Coulomb criterion and global equilibrium. The factor by which the shear strength parameters must be reduced in order to reach this critical failure condition, is the classical factor of safety of the slope, FS.

EXAMPLE PROBLEMS

Finite element stability analyses have been performed on homogeneous slopes consisting of the two soil types indicated in Table IV. The table indicates only those parameters of primary concern for finite element slope stability analysis. Secondary parameters, such as Young's modulus, Poisson's ratio and the dilation angle are given the nominal values of $E = 10^5$ kPa, $v = 0.3$ and $\psi = 0$, respectively, in both cases.

[‡] In this study four Gauss points are defined within each element.

Table IV. Soil types and properties considered in slope stability analyses.

Soil type	n	α (kPa^{-1})	ϕ' (deg)	c' (kPa)	γ (kN/m^3)
Silt	4	0.05	30	5	20
Clay	1.7	0.005	20	10	20

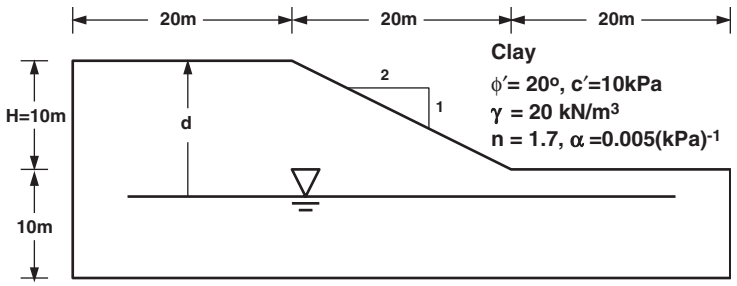

(a)

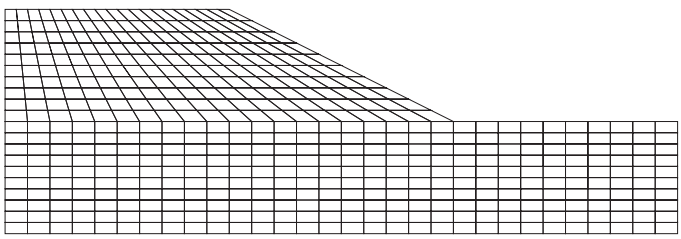

(b)

Figure 8. Clay slope: (a) Geometry and soil properties; and (b) FE discretization.

Two sets of runs were performed on each slope. In the first set, with no infiltration ($Q = 0$), the influence on stability of a horizontal water table at various depths (d) beneath the crest of the slope was investigated.

In the second set, for a fixed value of the water table depth d, the influence on stability of different infiltration/evaporation levels was investigated. In all cases, the factor of safety of the slope was plotted against the variable d or Q.

Clay slope analysis

The clay slope and its finite element discretization are shown in Figures 8(a) and 8(b). The slope has a factor of safety of FS = 1.37 using Bishop's method when assuming a deep water table, and FS = 1.78 when fully submerged. For the case of no infiltration ($Q = 0$), results from the finite element analyses with varying d, both with and without the inclusion of suction stresses, are shown in Figure 9(a). Considering first the line corresponding to 'No suctions', it is seen that the factor of safety varies from 1.78 for a fully submerged slope, to 1.36 for a 'dry' slope with a deep water table. The close agreement with the limit equilibrium solutions should be noted. The critical pool level that gives the minimum factor of safety of FS $\approx$ 1.27 occurs at

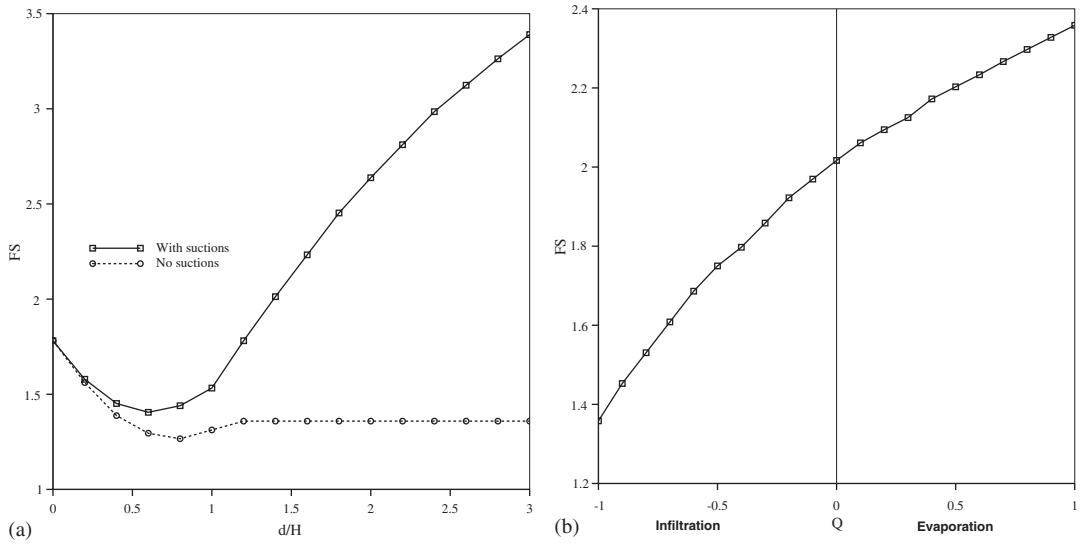

Figure 9. (a) Clay slope. Influence of the free-surface depth on the factor of safety with no infiltration ($Q = 0$). Both suction and no-suction cases considered; and (b) clay slope. Influence of the infiltration rate Q on the factor of safety with the free-surface depth fixed at $d/H = 1.4$ ($d = 1.4$ m).

$d/H \approx 0.8$ ($d \approx 8$ m), is an interesting phenomenon that has been noted by others (e.g. Reference [7]). When the suction stress function from Equation (15) is included in the analysis, the factor of safety minimum still occurs (increased to FS ≈ 1.41), however after passing the minimum, as the water table depth further increases, the factor of safety also consistently increases. The explanation lies in the nature of the suction stress function for fine-grained soils. From Figure 6(a), it can be seen that the case considered here with $Q = 0$ is at the boundary of Regimes III and IV. The dimensionless suction stress is seen to increase indefinitely with depth above the water table, leading to greater soil strength in the slope, and an increasing factor of safety.

For the same slope, and with the water table depth fixed at $d/H = 1.4$ ($d = 14$ m), Figure 9(b) gives the variation of the factor of safety with the infiltration rate Q. The figure indicates that the factor of safety consistently increases as the infiltration level decreases and the evaporation level increases. Referring again to Figure 6(a), it can be seen that when $Q \geqslant 0$, the analysis lies in Regime IV, and there exists a limiting depth at which the suction stresses tend to infinity. This limit is also shown clearly in Figure 5(b). It is instructive to find the limiting depth for the particular geometry considered here. The depth of the water table beneath the crest of the slope is given by $d = 14$ m, thus for a soil with $\alpha = 0.005\ \text{kPa}^{-1}$, the limiting dimensionless depth to the crest is given by, $Z_{\text{limit}} = 0.6867$ ($\gamma_w = 9.81\ \text{kN/m}^3$). The maximum evaporation rate that will result in real suction stress values within the slope is therefore given from Equation (20) as $Q = 1.0130$. The range of Q-values plotted in Figure 10(b), goes up to an evaporation level of $Q = 1.0$, and thus falls just short of the limiting value. If a value of Q greater than this limiting value is input to the analysis, a warning flag is generated stating that the suction stress is undefined within some upper regions of the slope.

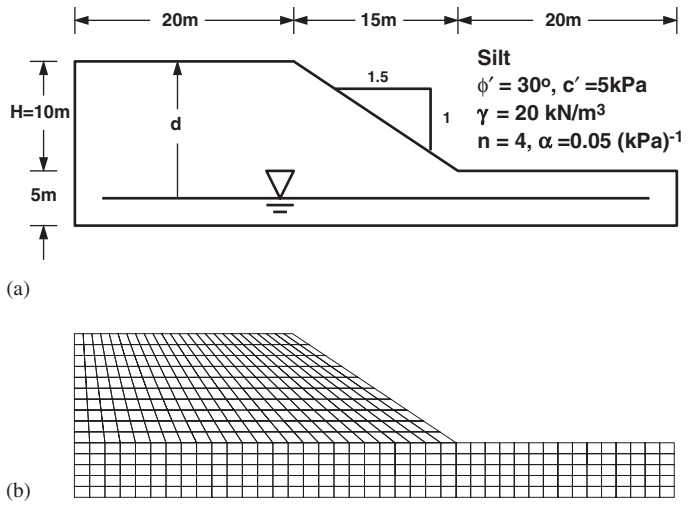

Figure 10. Silt slope: (a) Geometry and soil properties; and (b) FE discretization.

Silt slope analysis

The silt slope and its finite element discretization are shown in Figures 10(a) and 10(b). The reduced foundation depth used in this mesh, as compared with the clay slope from Figure 8(b), was in the interests of computational economy. It was observed in preliminary studies, that the failure mechanisms for the silt slope, both with and without suctions, never fell below the toe, whereas the clay slope exhibited deeper failure mechanisms.

The silt slope has a factor of safety of FS = 1.29 using Bishop's method when assuming a deep water table, and FS = 1.54 when fully submerged. For the case of no infiltration ($Q = 0$), results from the finite element analyses with varying d, both with and without the inclusion of suction stresses, are shown in Figure 11(a). Considering first the line corresponding to 'No suctions', it is seen that the factor of safety varies from 1.50 for a fully submerged slope, to 1.23 for a 'dry' slope with a deep water table. As before, good agreement with the limit equilibrium solutions is obtained, and a minimum factor of safety of FS $\approx$ 1.16 is observed at $d/H \approx 0.8$ ($d \approx 8$ m). With the inclusion of suction stresses from Equation (15), a minimum in the factor of safety variation is still observed (increased to FS = 1.25), however after passing the minimum, and as the water table depth further increases, the factor of safety rises to a maximum of FS $\approx$ 1.47 at $d/H \approx 1.1$ ($d \approx 11$ m), before falling back to the 'dry' solution of FS = 1.23.

The explanation lies in the nature of the suction stress function for coarser-grained soils. From Figure 7(a), it can be seen that the case considered here with $Q = 0$ is at the boundary of Regimes I and II. The dimensionless suction stress is seen to reach a pronounced maximum at a dimensionless depth above the water table given by Equation (19) ($Q = 0$) to be $Z_{\max} = 0.8409$. Thus for a soil with $\alpha = 0.05$ kPa^{-1}, the actual depth of the maximum suction stress occurs $z_{\max} = 1.7144$ m above the water table. The maximum factor of safety was observed when $d \approx 11$ m, thus for a slope of height $H = 10$ m the maximum suction stress is at, or just above the toe of the slope, where the suctions are most effective in stabilising the slope and increasing the factor of safety.

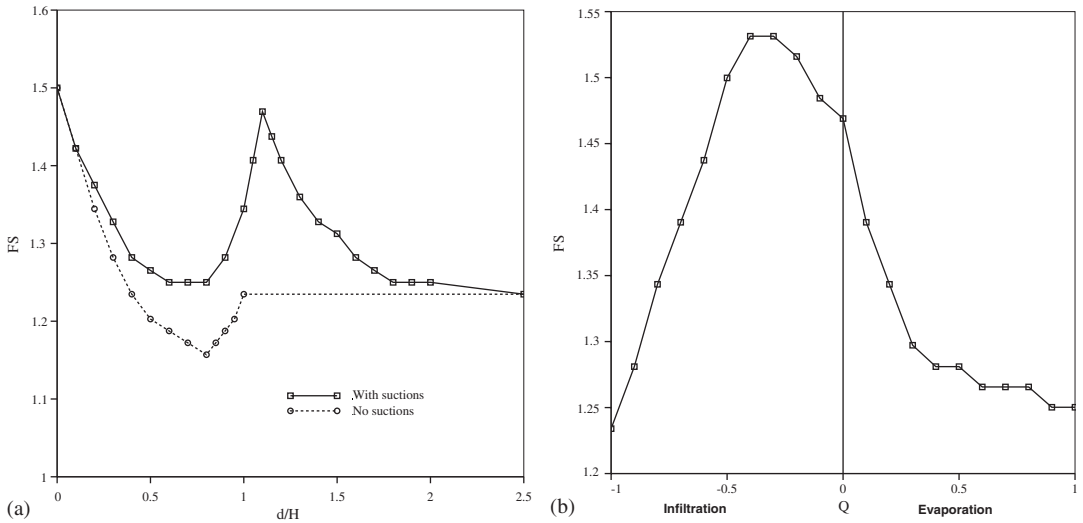

Figure 11. (a) Silt slope. Influence of the free-surface depth on the factor of safety with no infiltration ($Q = 0$). Both suction and no-suction cases considered; and (b) silt slope. Influence of the infiltration rate Q on the factor of safety with the free-surface depth fixed at $d/H = 1.1$ ($d = 11$ m).

For the same slope, and with the water table depth fixed at $d/H = 1.1$ ($d = 11$ m), Figure 11(b) gives the variation of the factor of safety with the infiltration rate Q. The figure indicates that the factor of safety reaches a pronounced peak of FS ≈ 1.53 when the infiltration rate is given by $Q \approx -0.3$. Bearing in mind that the factor of safety of this slope with suction stresses but no infiltration, was about 1.47, this result suggests that a modest amount of infiltration, moving the solution into Regime II as shown in Figure 7(a), will *increase* the factor of safety for the particular slope considered. Further increase of the infiltration rate towards its theoretical maximum of $Q = -1$, moves the solution into Regime III, and gradually removes all suctions from the soil profile. The absence of suction stresses naturally causes the factor of safety to fall back to the 'dry' soil solution mentioned above.

Increased evaporation ($Q > 0$) in this example moves the solution into Regime I and also causes the factor of safety to fall to the 'dry' solution. The explanation of this trend is shown in Figure 7(a), where it is seen that as the evaporation level increases, the peak suction stress occurs ever closer to the water table and falls very rapidly back to zero. Thus at high evaporation levels ($Q \to 1$), and with the water table below the toe of the slope, the suction stresses reach their peak and return to zero before they have a chance to impact on the stability of the slope.

Finally, Figure 12 shows the deformed finite element mesh at failure for the silt slope, both with and without suctions above the water table. In both cases, the water table is fixed at $d/H \approx 1.1$ ($d \approx 11$ m), which was chosen because it results in the maximum FS $= 1.47$ value with suctions as shown in Figure 11(a). The slope without suctions however, gave a lower factor of safety of FS $= 1.23$, corresponding to a conventional toe failure as shown in Figure 12(b). A comparison of the two figures shows quite clearly how the suctions close to the toe of the slope in case (a), have strengthened the soil in this vicinity, and pushed the failure mechanism away from the toe. The deformed mesh in Figure 12(a), indicates a slope failure, with the mechanism outcropping some distance above the toe.

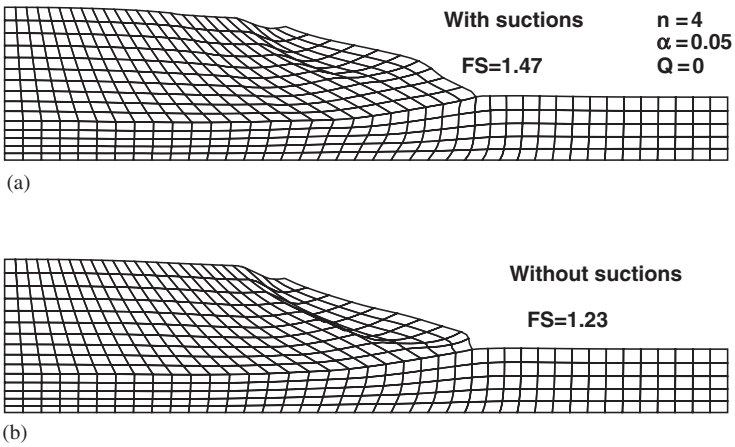

Figure 12. Failure mechanisms from finite element analysis of the silt slope with no infiltration: (a) with suctions; and (b) without suctions above the water table. In both cases the water table is at $d = 11$ m.

CONCLUDING REMARKS

A general framework for slope stability analysis of unsaturated soils has been presented by combining a model for suction stresses above the water table with elasto-plastic finite elements. The framework is implemented within the context of classical effective stress theory. The suction stress profile in unsaturated soil is fully described by a knowledge of the matric suction and the suction stress coefficient χ which in this paper has been defined as being equal to the equivalent degree of saturation.

The suction stress profile depends on three soil parameters, the saturated hydraulic conductivity k_s and pore size parameters α and n, and a steady infiltration or evaporation rate q.

When applied to slope stability problems with a water table, different soils exhibit quite different stability characteristics when implementing the suction stress theory. The factor of safety of a slope depends not only on the water table location and the soil type, but also the evaporation or infiltration rate.

In a clay slope, evaporation enhances the factor of safety, while infiltration decreases it. In a silt slope however, the influence of evaporation or infiltration is more complex. High infiltration or high evaporation both cause the factor of safety to fall, however at intermediate values, the factor of safety reaches a maximum, corresponding either to a state of infiltration or evaporation, depending on the depth of the water table.

When compared with the classical factor of safety in which suctions are ignored, the impact of suctions is more significant in clays than silts. In a clay slope with suctions, as the depth of the water table drops below the toe of the slope, the factor of safety continually increases. Without suctions however, the factor of safety levels out once the water table falls below a depth at which it has no further influence on the effective stresses in the potential sliding mass.

In a silt slope with suctions, a maximum factor of safety is observed when the water table is at a depth that gives maximum suctions stresses in the vicinity of the toe of the slope. The

maximum is observed to be 20–30% higher than the minimum value that occurs without suctions when the water table is situated at approximately one third of the slope height above the toe. A decreasing trend is observed in the factor of safety with suctions as the water table depth is further increased. In this case the suction stresses are peaking and reducing to zero below the toe of the slope and are thus having no impact on stability. At significant water table depths, the factors of safety both with and without suctions are essentially the same.

The powerful methodology described in this paper, in which suction stress theory is combined with elasto-plastic finite elements, has many applications in geotechnical analysis. Further studies are planned to investigate the influence of suctions above an inclined free-surface on slope stability, in addition to investigations on the impact of suction stresses on other geotechnical stability problems, such as bearing capacity and earth pressure analysis.

NOMENCLATURE

c'	effective cohesion
d	depth of water table below crest of slope
FS	slope factor of safety
H	height of slope
h	total head
k	unsaturated permeability
k_s	saturated permeability
n	pore size exponent
q	steady flow rate per unit area (infiltration negative)
Q	dimensionless flow rate (q/k_s)
U	dimensionless suction stress ($\alpha\chi(u_a - u_w)$)
U_{limit}	limiting value of U
U_{max}	maximum value of U
u_a	air pressure
u_w	suction pore pressure
$(u_a - u_w)$	matric suction
Z	dimensionless depth ($\alpha\gamma_w z$)
Z_{limit}	limiting value of Z
Z_{max}	maximum value of Z
z	height above the water table
α	inverse of air entry value
γ	soil unit weight
γ_w	water unit weight
σ	total stress
σ'	effective stress
τ	shear stress
τ_f	shear strength
ϕ'	effective friction angle
χ	matric suction coefficient
ψ	pressure head

ACKNOWLEDGEMENTS

The writers acknowledge the support of NSF Grant No. CMS 97-13442.

REFERENCES

1. Tsaparas I, Rahardjo H, Toll DG, Leong EC. Controlling parameters for rainfall induced landslides. *Computers and Geotechnics* 2002; **29**(1):1–27.
2. Cho SE, Lee SR. Instability of unsaturated slopes due to infiltration. *Computers and Geotechnics* 2001; **28**(3): 185–208.
3. Rahardjo H, Leong EC. Soil–water characteristic curves and flux boundary problems. In *Unsaturated Soil Engineering Practice*, Houston SL *et al* (eds). Geotechnical Specialty Publication No. 68. ASCE: New York, 1997; 89–111.
4. Fredlund DG, Rahardjo H. *Soil Mechanics for Unsaturated Soils*. Wiley: Chichester, NY, 1993.
5. Krahn J, Fredlund DG, Klassen MJ. Effect of soil suction on slope stability at Notch Hill. *Canadian Geotechnical Journal* 1989; **26**:269–278.
6. Freeze RA, Cherry JA. *Groundwater*. Prentice-Hall: Englewood Cliffs, NJ, 1979.
7. Griffiths DV, Lane PA. Slope stability analysis by finite elements. *Géotechnique* 1999; **49**(3):387–403.
8. Bishop AW. The principle of effective stress. *Teknsik Ukeblad* 1955; **106**(39):859–863 (Lecture delivered in Oslow, Norway).
9. Bishop AW. The use of pore pressure coefficients in practice. *Géotechnique* 1954; **4**(2):148–152.
10. Blight GE. Strength and consolidation characteristics of compacted soils. *Ph.D. Thesis*, University of London, U.K., 1961.
11. Donald IB. The mechanical properties of saturated and partly saturated soils with special reference to negative pore water pressure. *Ph.D. Thesis*, University of London, U.K., 1961.
12. Escario V, Juca J. Strength and deformation of partly saturated soils. *Proceedings of the 12th International Conference on Soil Mechanics and Foundation Engineering*, vol. 3, 1989; 43–46.
13. Vanapalli SK, Fredlund DG. Comparison of different procedures to predict unsaturated soil shear strength. In *Advances in Unsaturated Geotechnics*, Shackelford CD *et al* (eds). Geotechnical Specialty Publication No. 99. ASCE: New York, 2000; 195–209.
14. Gardner WR. Steady state solutions of the unsaturated moisture flow equation with application to evaporation from a water table. *Soil Science* 1958; **85**:228–232.
15. Phillips JR. The quasi-linear analysis, the scattering analog and other aspects of infiltration and seepage. In *Infiltration Development and Application*, Fok YS (ed.). Water Resources Research Center of the University of Hawaii, 1987; 1–27.
16. Yeh T-CJ. One-dimensional steady state infiltration in heterogeneous soils. *Water Resources Research* 1989; **25**(10):2149–2158.
17. Stephens DB. *Vadose Zone Hydrology*. CRC Press: Boca Raton, 1995.
18. Singh VP. *Kinematic Wave Modeling in Water Resources*. Wiley: Chichester, NY, 1997.
19. van Genuchten MY. A closed form equation for predicting the hydraulic conductivity of unsaturated soils. *Soil Science Society of America Journal* 1980; **44**:892–898.
20. Bishop AW, Blight GE. Some aspects of effective stress in saturated and partly saturated soils. *Géotechnique* 1963; **13**(3):177–197.
21. Vanapalli SK, Fredlund DG, Pufahl DE, Clifton AW. Model for the prediction of shear strength with respect to soil suction. *Canadian Geotechnical Journal* 1996; **33**:379–392.
22. Oberg A, Sallfors G. Determination of shear strength parameters of unsaturated silts and sands based on the water retention curve. *Geotechnical Testing Journal, ASTM* 1997; **20**(1):40–48.
23. Khalili N, Khabbaz MH. A unique relationship for χ for the determination of the shear strength of unsaturated soils. *Géotechnique* 1998; **48**(5):681–687.
24. Lu N, Likos WJ. *Unsaturated Soil Mechanics*. Wiley: Hoboken, NJ, 2004.
25. Bear J. *Dynamics of Fluids in Porous Media*. Elsevier: Amsterdam, 1975.
26. Marshall TJ, Holmes JW, Rose CW. *Soil Physics* (3rd edn). Cambridge University Press: Cambridge, U.K., 1996.
27. Smith IM, Griffiths DV. *Programming the Finite Element Method* (4th edn). Wiley: Chichester, NY, 2004.

